ACS APPLIED MATERIALS & INTERFACES

Research Article

www.acsami.org

Polydopamine-Coated Porous Substrates as a Platform for Mineralized β-FeOOH Nanorods with Photocatalysis under Sunlight

Chao Zhang, Hao-Cheng Yang, Ling-Shu Wan,* Hong-Qing Liang, Hanying Li, and Zhi-Kang Xu*

MOE Key Laboratory of Macromolecular Synthesis and Functionalization, Department of Polymer Science and Engineering, Zhejiang University, Hangzhou 310027, People's Republic of China

Supporting Information

ABSTRACT: Immobilization of photo-Fenton catalysts on porous materials is crucial to the efficiency and stability for water purification. Here we report polydopamine (PDA)-coated porous substrates as a platform for in situ mineralizing β-FeOOH nanorods with enhanced photocatalytic performance under sunlight. The PDA coating plays multiple roles as an adhesive interface, a medium inducing mineral generation, and an electron transfer layer. The mineralized β-FeOOH nanorods perfectly wrap various porous substrates and are stable on the substrates that have a PDA coating. The immobilized β-FeOOH nanorods have been shown to be efficient for degrading dyes in water via a photo-Fenton reaction. The degradation efficiency reaches approximately 100% in 60 min when the reaction was carried out with H_2O_2 under visible light, and it remains higher than 90% after five cycles. We demonstrate that the PDA coating promotes electron transfer to reduce the electron−hole recombination rate. As a result, the β-FeOOH nanorods wrapped on the PDA-coated substrates show enhanced photocatalytic performance under direct sunlight in the presence of H_2O_2. Moreover, this versatile platform using porous materials as the substrate is useful in fabricating β-FeOOH nanorods-based membrane reactor for wastewater treatment.

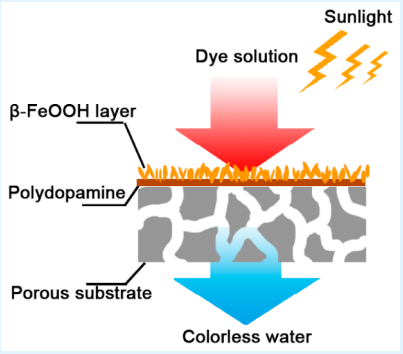

KEYWORDS: *β-FeOOH nanorods, mineralization, polydopamine, photo-Fenton, porous materials*

1. INTRODUCTION

Advanced oxidation processes (AOPs), including electrochemical catalysis,[1] semiconductor photocatalysis,[2] and Fenton/photo-Fenton reactions,[3] have shown great potential in wastewater treatment. Among them, heterogeneous photo-Fenton reaction is an effective and commonly used method to degrade organic pollutants in wastewater.[4] However, this reaction is usually carried out with heterogeneous photocatalysts suspended in slurry reactors. The suspended photocatalysts are relatively insufficient to harvest light energy, resulting in low photocatalytic activity.[5] They also need to be recycled with additional processes for continuous use, and may leak out and cause secondary pollution.

The photo-Fenton catalysts can be immobilized on inorganic[6] or organic substrates[7,8] for practical applications. Immobilization of photocatalysts on separation membranes by surface engineering strategies is very promising for photocatalytic membrane reactors toward wastewater treatment.[9] The membranes play multiple roles through harvesting light for effective photo-Fenton reaction and purifying water by filtration. For example, Nafion membrane was exchanged with Fe ion and used to degrade nonbiodegradable azo dye in the presence of H_2O_2.[10] However, polymer membranes are usually hydrophobic, inert, and nonadhesive for catalyst immobilization. Preprocesses, such as UV grafting[11] and plasma treatment,[12−14] must be used to activate the membrane surfaces, which generally affect the porous structure, separation performance, and mechanical strength of the membranes. On the other hand, the heterogeneous photocatalysts usually have low efficiency because the electron−hole recombination rate is too high in a photo-Fenton reaction.[15] Some strategies, including metal/nonmetal doping[16] and semiconductor[17] or electron acceptor coupling,[18] were developed to reduce the electron−hole recombination rate, and then to enhance the catalytic efficiency. Nevertheless, they are not facile to be integrated on/in polymer membranes and membrane reactors for wastewater treatment. Therefore, it remains a major challenge for rationally designing a universal approach to stably immobilize photocatalysts on membrane surfaces, to effectively reduce the electron−hole recombination rate, and then to efficiently enhance the photocatalytic activity in a photo-Fenton reaction.

Dopamine has been used as a versatile chemical for the surface engineering of polymer membranes in recent years.[19−21] It is very interesting that polydopamine (PDA) can be used as an intermediary for surface mineralization to generate and immobilize nanosized minerals on the membrane surfaces.[22−24] These nanosized minerals do not impact the porous structures of polymer membranes for microfiltration. They endow the membranes with superhydrophilicity, underwater superoleophobicity, high water permeation flux, and high separation efficiency for oil/water mixtures. Most recently, it has been

Received: March 22, 2015
Accepted: May 13, 2015
Published: May 13, 2015

DOI: 10.1021/acsami.5b02530
ACS Appl. Mater. Interfaces 2015, 7, 11567−11574

found that PDA is able to act as an electron acceptor to promote electron transfer,[25,26] which will be advantageous for photo-Fenton reactions. In this work, therefore, we report the in situ mineralization of β-FeOOH nanorods using PDA-coated porous substrates as a platform, which include porous meshes and microfiltration membrane, and demonstrate the application in water purification under sunlight. β-FeOOH is a rather promising heterogeneous photo-Fenton catalyst because it has a band gap of 2.12 eV to effectively harvest sunlight.[27−29] Our approach results in highly uniform and stably immobilized β-FeOOH nanorods on the platform surfaces, providing as many photocatalytic sites as possible to degrade dyes in wastewater via the photo-Fenton reaction in the presence of H_2O_2. The PDA-mediated β-FeOOH nanorods show greatly enhanced photocatalytic performance and excellent recyclability for dye degradation under sunlight. To the best of our knowledge, this is the first time to use PDA as an adhesive interface, a medium inducing mineral generation, and an electron transfer layer to form an effective platform for in situ mineralizing nanosized catalysts on porous materials.

2. EXPERIMENTAL SECTION

Materials. Commercial porous materials were used as the substrates, which include polypropylene nonwoven (PPNW), polypropylene microfiltration membrane (PPMM), nylon mesh, and polyester cloth. All substrates were cut into disks with a diameter of 45 mm, washed by acetone overnight to remove impurities, and then dried in a vacuum oven at 30 °C. Dopamine hydrochloride was purchased from Sigma-Aldrich. Other reagents, such as ironchloride hexahydrate, tris-(hydroxymethyl) aminomethane, methyl orange, rhodamine B, methyl blue, methylene blue, ethanol, and hydrochloric acid, were received from Sinopharm Chemical Reagent Co., Ltd. and used without further purification. Water used in all experiments was deionized and ultrafiltrated to 18.2 MΩ with an ELGA LabWater system (France).

Preparation of PDA-Coated Porous Substrates. Dopamine hydrochloride (2 mg/mL) was dissolved in Tris buffer solution (pH 8.5, 50 mM). Porous substrates were prewetted by ethanol and then immersed in the buffer solution with shaking in the air oscillator for 8 h at 25 °C. Subsequently, the PDA-coated substrates were washed by water for 4 h and dried in a vacuum overnight at 30 °C.

Mineralization of β-FeOOH Nanorods on PDA-Coated Substrates. $FeCl_3·6H_2O$ (0.067 M) was added to a mixed solution of deionized water (20 mL) and hydrochloric acid (10 mL, 0.01 M), in which the PDA-coated substrates were immersed and kept at 60 °C for 24 h. The samples were taken out, washed with deionized water for 4 h, and dried in a vacuum at 30 °C for another 4 h.

Characterization. Morphology of the samples was observed by field emission scanning electron microscope (FESEM, Hitachi S4800, Japan). X-ray photoelectron spectra were collected by a spectrometer (XPS, PerkinElmer, Waltham, MA) with Al Kα excitation radiation (1486.6 eV). FT-IR/ATR spectra were conducted on an infrared spectrophotometer (Nicolet 6700) equipped with an ATR accessory (ZnSe crystal, 45°). UV−vis diffuse reflectance spectra (DRS) were recorded with a UV−vis spectrophotometer (\UV-2401, Shimadzu, Japan) by using $BaSO_4$ as the reference. UV−vis absorption of the solutions was measured with an ultraviolet spectrophotometer (UV 2450, Shimadzu, Japan). Photoluminescence spectrometer (FLS920, Edinburgh instruments) with Xe lamp (450 W, 325 nm) was used as the excitation source.

Photocatalysis Measurement. The photocatalytic performance of the β-FeOOH nanorods wrapped substrates was evaluated by degrading different dyes in water under visible lights generated by a 500 W Xe lamp equipped with a cutoff filter of 420 nm or under sunlight (30 °C and 15% RH). Before visible light or sunlight irradiation, the β-FeOOH nanorods wrapped platforms were added to an aqueous solution of dye (25 mL, 20 mg/L, pH 3), and shaken in the dark for 30 min to reach an adsorption−desorption equilibrium. After measuring the initial concentration (C_0), H_2O_2 (9.8 mM) was immediately added into the solution. During visible light irradiation, 1 mL of the solution was taken out and diluted to 3 mL to measure the dye concentration (C_t) at different times. For the experiments under sunlight, the concentrations of the dyes (15 mL, 20 mg/L, pH 3) were measured before and after the photo-Fenton reaction to calculate the degradation efficiency.

3. RESULTS AND DISCUSSION

Figure 1 illustrates the process of mineralizing and immobilizing β-FeOOH nanorods using PDA-coated substrates as a platform. First, porous substrates, such as PPNW, PPMM, polyester cloth, and nylon mesh, were immersed in dopamine solution at room temperature to form uniform PDA coating on their surfaces. The substrates turn to brown or black after 8-h deposition without major changes in their morphologies and structures (Figure S1 in the Supporting Information (SI)). Then, yellow FeOOH nanorods were mineralized on the PDA-coated substrates by a hydrolysis reaction. The PDA coating plays a crucial role during this process because the iron ions are captured via catechol chelation to form nucleation sites for mineralization and immobilization.[30] The mineralized FeOOH nanorods are relatively stable on the substrates after 112 h washing with deionized water at a shaking rate of 90 rpm in an oscillator (Figure S2, SI). This strategy is available to other porous or dense materials such as silicon, glass, and ceramics, because PDA has been demonstrated to be able to form coatings on various substrates.[31]

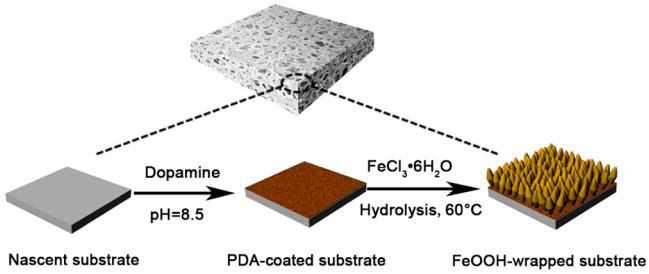

Figure 1. Schematic illustration for the fabrication process of β-FeOOH nanorods on PDA-coated substrates.

FESEM was used to characterize the mineralized FeOOH on the PDA-coated substrates. FeOOH nanorods can be synthesized by using some shape-control agents including dopamine.[32] Compared to those on the nascent PPNW without PDA coating (Figure S3, SI), FeOOH nanorods wrap the PDA-coated platforms uniformly (Figure 2), which can protect the polymer substrates from degradation during the photo-Fenton reaction.[33] FeOOH nanorods gradually wrap the fibers (Figure S4, SI) and the mineral content increases from 5% to 11% (Figure S5, SI) with the increase of mineralization time from 6

DOI: 10.1021/acsami.5b02530
ACS Appl. Mater. Interfaces 2015, 7, 11567−11574

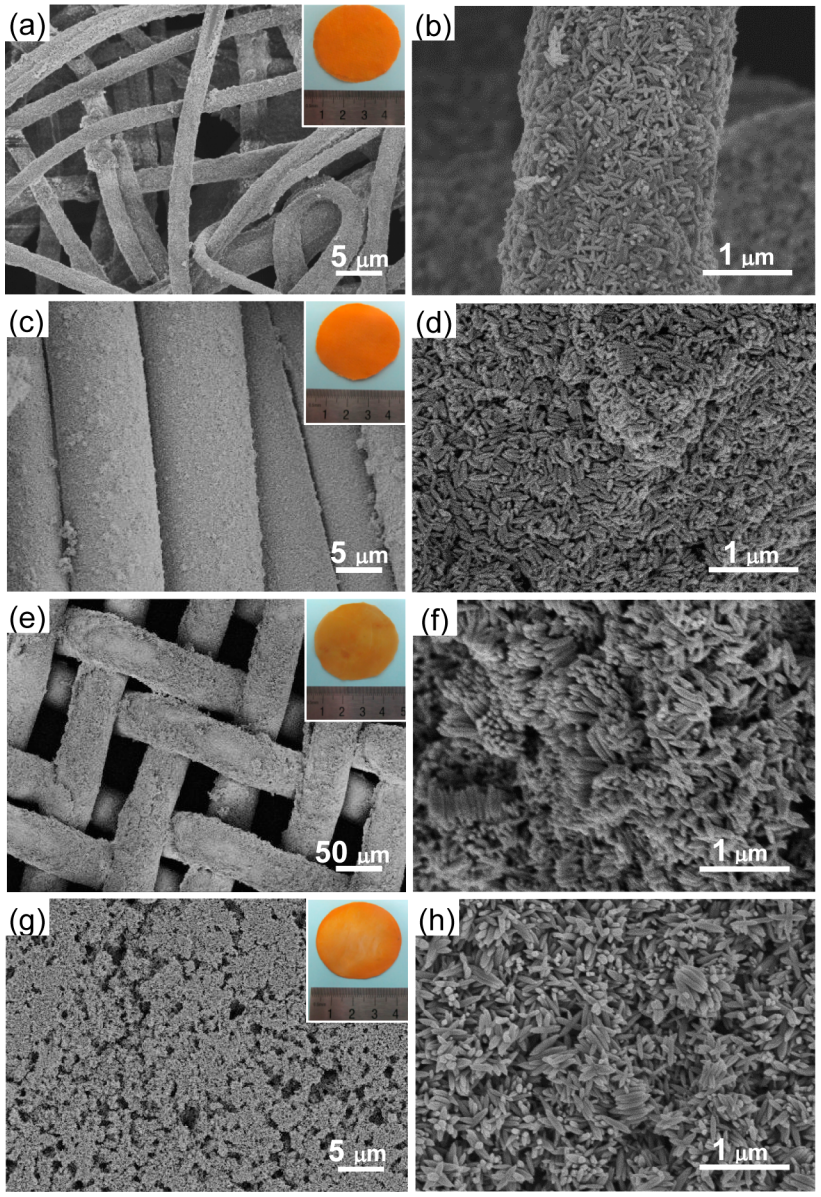

Figure 2. FESEM images (×30 000) of the mineralized β-FeOOH nanorods on different PDA-coated substrates. (a,b) PPNW, (c,d) polyester cloth, (e,f) nylon mesh, and (g,h) PPMM. The insets are digital images of the samples.

to 24 h. The properties of the substrates slightly affect the size and morphology of FeOOH nanorods. For example, the size of FeOOH nanorods increases from 180 × 60 ± 20 × 8 nm to 400 × 140 ± 22 × 10 nm with the fiber radius of PPNW, polyester cloth, and nylon mesh (Table S1, SI). Moreover, some nanorods aggregate on the fiber surface. For PPMM, on the other hand, the nanorods are mainly decorated on the outer surface because the membrane pores (~200 nm) are smaller than the mineralized nanorods (370 × 110 ± 30 × 15 nm). The resulted small pores are advantageous for water purification by filtration. On the other hand, the mineralized nanorods have slight effect on the tensile strength but markedly decrease the break elongation as compared to the nascent PPMM (Figure S6, SI). These results indicate that the porous substrates become fragile after mineralization.

XRD, FT-IR and XPS were used to analyze the chemical structures and crystal phase of the mineralized FeOOH nanorods on the porous substrates. Diffraction peaks appear at 12° (110), 26.9° (310), 35.4° (211), 39.4° (301), and 56.2° (521) (Figure 3A), revealing β-FeOOH (JCPDS No. 34−1266). FT-IR spectra (Figure 3B) show a broad peak between 3500 and 3100 cm^{-1} attributed to the stretching vibrations of N−H and O−H in the PDA coating, which also has a weak absorption peak at 1608 cm^{-1} for the C═C stretching vibration of aromatic ring.[20] Peaks at 3340 and 837 cm^{-1} are due to the O−H and Fe−O stretching vibrations in β-FeOOH, respectively.[34] The chemical composition was also revealed by XPS spectra (Figure 3C and D). Two signals appear from O_{1s} and N_{1s} at the PDA-coated platform surfaces, and the N/O ratio is 0.4 (the theoretical value is 0.5). Signals at 724.2 and 710.8 eV are the characteristic peaks from $Fe_{2p1/2}$ and $Fe_{2p3/2}$ in β-FeOOH.[35] All the results indicate that β-FeOOH nanorods have been mineralized on the PDA-coated substrates. It is well-known that β-FeOOH can be used as a heterogeneous photo-Fenton catalyst for dye degradation.[27−29] As a result, the nanorods wrapped PDA-coated porous substrates should combine the photocatalytic performance with the filtration characteristics.

DOI: 10.1021/acsami.5b02530
ACS Appl. Mater. Interfaces 2015, 7, 11567−11574

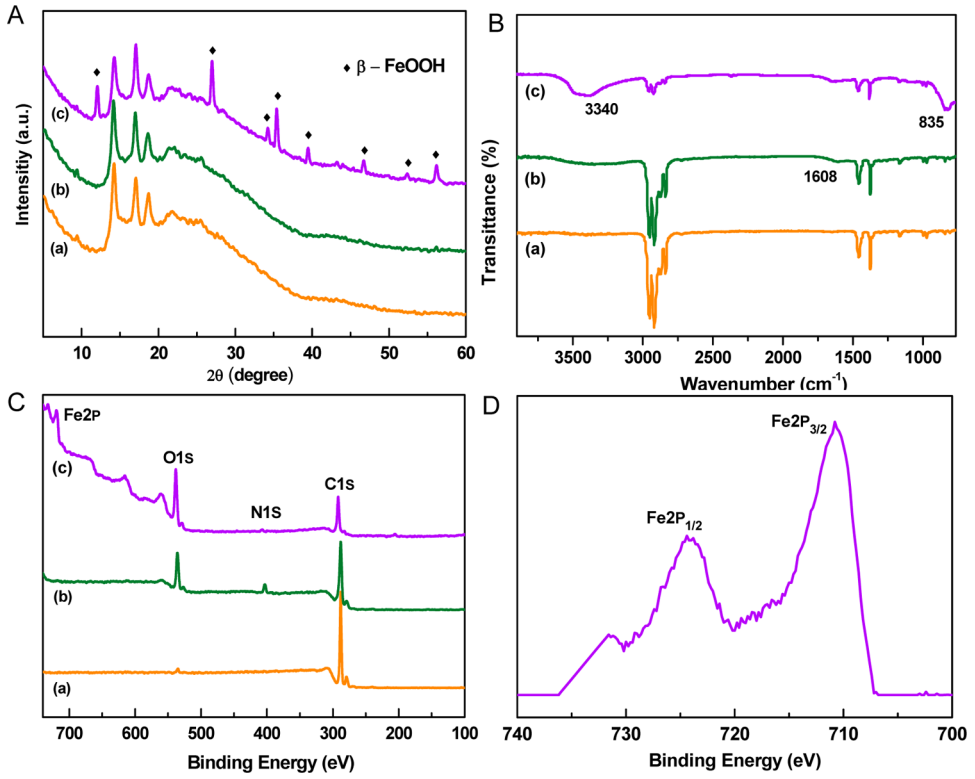

Figure 3. (A) XRD patterns, (B) ATR/FT-IR spectra, (C) XPS spectra of the nascent (a), PDA-coated (b), and *β*-FeOOH wrapped (c) PPNW. (D) XPS spectrum of core-level Fe 2p.

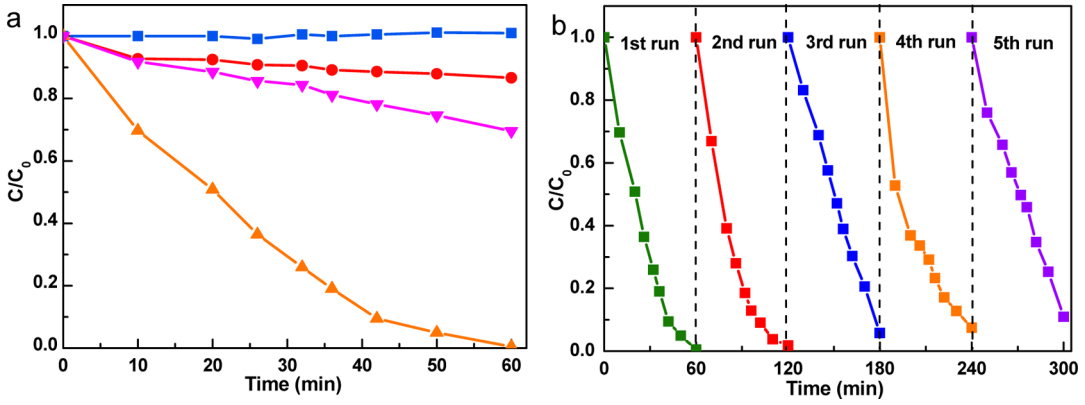

Figure 4. (a) Photocatalytic performance of the *β*-FeOOH nanorods wrapped PPNW for the degradation of methyl blue under visible light (λ > 420 nm) and in the dark at room temperature: (■) *β*-FeOOH nanorods wrapped PPNW under visible light, (●) H_2O_2 under visible light, (▼) *β*-FeOOH nanorods wrapped PPNW + H_2O_2 under dark, and (▲) *β*-FeOOH nanorods wrapped PPNW + H_2O_2 under visible light. (b) Reusability of the *β*-FeOOH nanorods wrapped PPNW in the photo-Fenton reaction. H_2O_2 was 9.8 mM at the beginning.

Methyl blue was degraded under visible light (λ > 420 nm) to evaluate the photocatalytic performance of the *β*-FeOOH nanorods wrapped substrates. Typical results are shown in Figure 4a. It can be seen that the *β*-FeOOH nanorods wrapped PPNW themselves can hardly degrade the dye under visible light within 60 min. Similarly, the degradation efficiency in visible light is only 13% even H_2O_2 was added. Nevertheless, it increases to approximately 100% when the reaction was carried out with H_2O_2 under visible light. In this case, a photo-Fenton process takes place, and the synergistic effect of H_2O_2 and visible light promotes the generation of tremendous amount of ·OH radicals,[36] which contribute to the degradation of methyl blue. The results also demonstrate that the *β*-FeOOH nanorods wrapped substrates are very efficient photo-Fenton catalysts under visible light. Some FeOOH-based materials have been reported for the photodegradation of organics in the presence of H_2O_2. For example, the degradation efficiency of 17*β*-estradiol (222 μg/L) reached 99.5% within 8 h irradiation in the presence of 5 g/L *β*-FeOOH/resin.[28] In addition, 90% of orange II (0.2 mM) was photodegraded within 7 h irradiation by copolymer-Fe_2O_3.[37] Our results are very promising considering the much short degradation time (~60 min), although direct comparison is not reasonable between the reported materials with the present photocatalysts because they are different in composition and shape. They have excellent reusability and stability to degrade methyl blue in the same condition. Figure 4b shows that the degradation efficiency maintains 90% after five cycles of photo-Fenton reaction. At the

DOI: 10.1021/acsami.5b02530
ACS Appl. Mater. Interfaces 2015, 7, 11567−11574

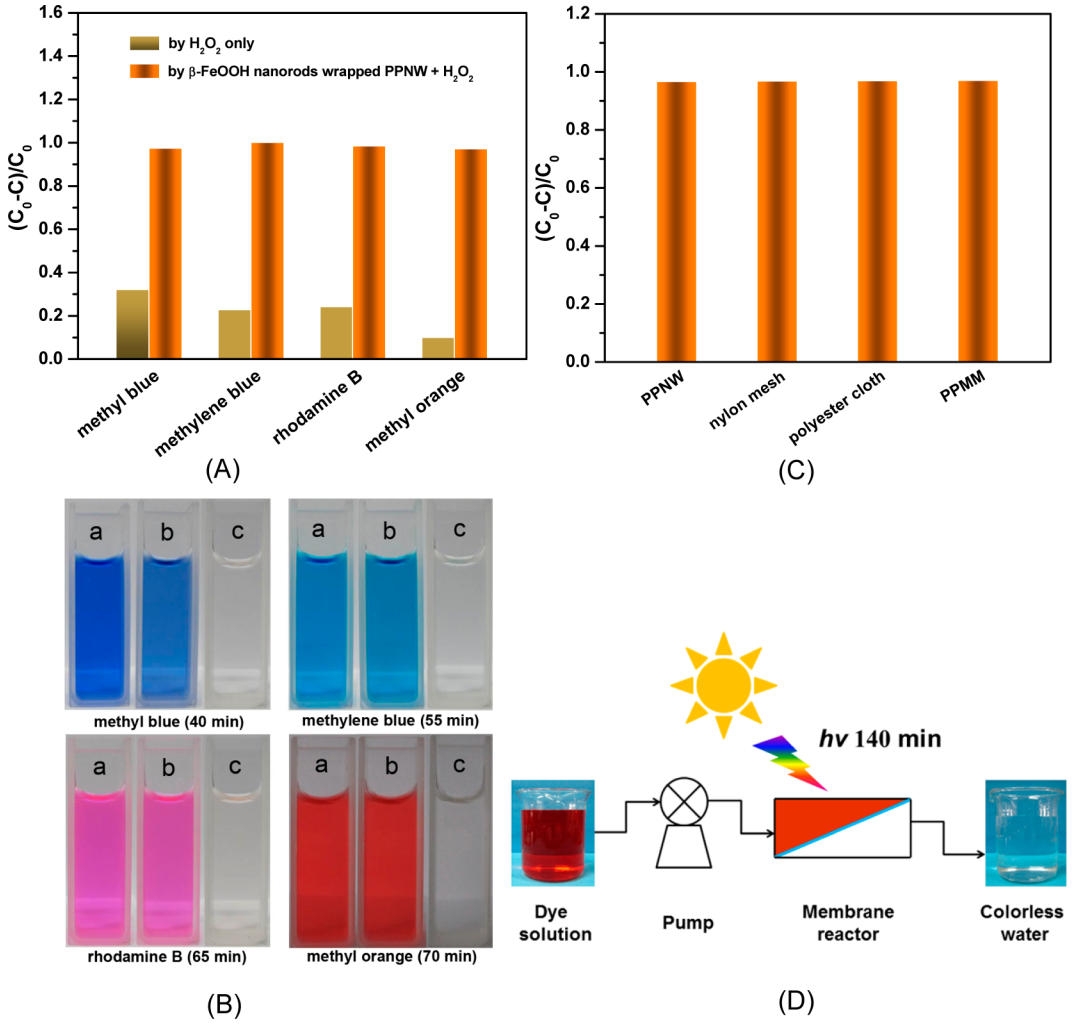

Figure 5. (A) Degradation efficiency of different dye solutions under sunlight at room temperature by the *β*-FeOOH nanorods wrapped PPNW. (B) Photographs of the dye solutions: (a) original, (b) degraded by H_2O_2 only, (c) degraded by *β*-FeOOH nanorods wrapped PPNW with H_2O_2. (C) Degradation efficiency of methyl orange under sunlight at room temperature by different *β*-FeOOH nanorods wrapped substrates. The degradation time is 70 min. (D) An intermittent membrane reactor for the degradation of methyl orange within 140 min under sunlight.

same time, the PDA-coated substrates are still completely wrapped by the *β*-FeOOH nanorods with stable morphology and crystal structure (SEM image in Figure S7 and XRD pattern in Figure S8 in the SI). The photocatalytic performance declines slightly with the increase of the cycle number of reuse. A possible reason is the deactivation of some photocatalytic sites.[38,39] As a whole, the *β*-FeOOH nanorods wrapped substrates show good stability in the process of photo-Fenton reaction.

In general, pH value, H_2O_2 concentration and catalyst content play key roles in the photo-Fenton reaction. The photocatalytic performance of *β*-FeOOH nanorods wrapped PPNW was measured at different pH values and H_2O_2 concentrations (Figure S9, SI). It can be seen that the property declines with the increase of pH value because little ·OH radicals are produced at high pH during the photo-Fenton.[40] The photocatalytic performance is enhanced when the H_2O_2 concentration increases from 3.9 to 9.8 mM. However, further increasing the concentration to 15.7 mM leads to a sharp decrease of the photocatalytic performance, which is due to the well-known hydroxyl radicals scavenging effect.[41,42] In addition, the content of *β*-FeOOH nanorods has a great influence on the photocatalytic performance (Figure S10, SI). The results show that long mineralization time results in increased catalytic nanorods and hence high photocatalytic performance.

The *β*-FeOOH nanorods wrapped substrates were also used to degrade other dyes, which are difficult to be eliminated from wastewater by traditional methods,[43,44] via the photo-Fenton reaction under direct sunlight. Figure 5A indicates that the degradation efficiency is higher than 97% within 40 min for methyl blue by the *β*-FeOOH nanorods wrapped PPNW. In fact, most of the dyes can be effectively degraded (Figure 5B), and the wastewater with methylene blue, rhodamine B or methyl orange, turns to colorless in 55, 65, and 70 min, respectively. Figure 5C shows that other *β*-FeOOH nanorods wrapped substrates have similar photocatalytic activity toward the studied dyes (Figure S11 in the SI).

It is well-known that slurry photocatalytic reactors have usually been designed and used, in which the photocatalysts must be recycled through filtration or flocculation. It is a cost- and time-consuming process, which hinders the large-scale application of the reactors. The substrates used in this work have porous structures for water filtration; therefore, an intermittent membrane reactor was designed to decompose dyes in wastewater (Figure 5D). Methyl orange (80 mL, 20 mg/L, pH 3) and H_2O_2 (9.8 mM) were mixed into the

DOI: 10.1021/acsami.5b02530
ACS Appl. Mater. Interfaces 2015, 7, 11567−11574

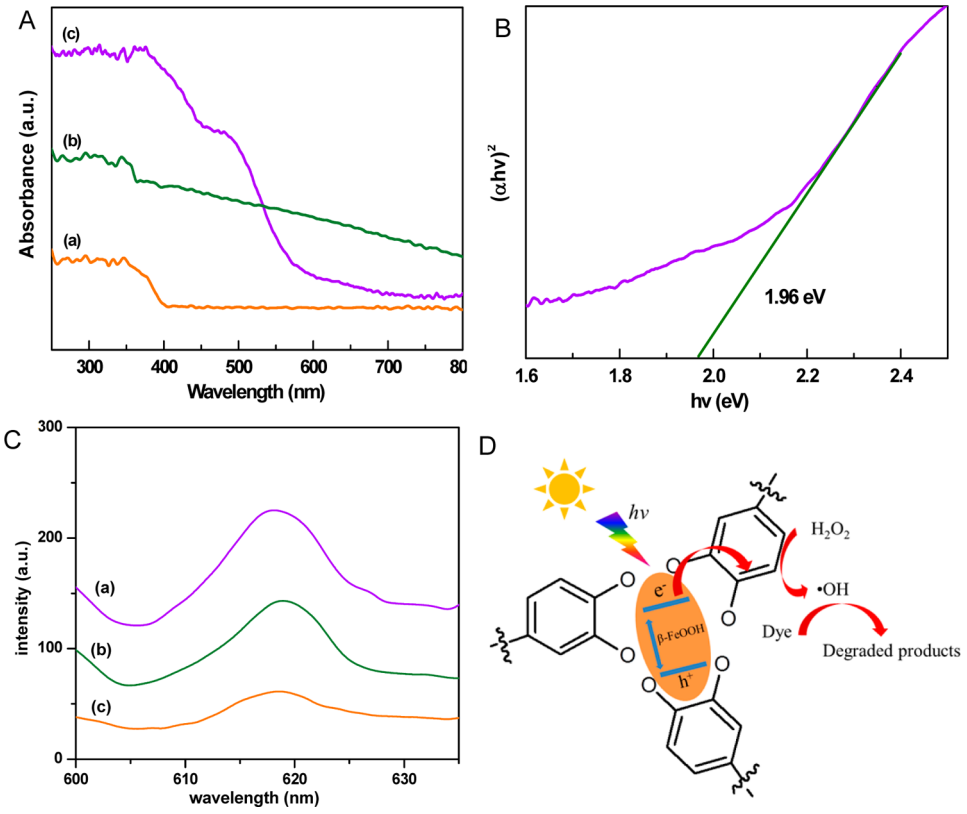

Figure 6. (A) UV−vis diffuse-reflectance spectra of the nascent (a), PDA-coated (b), andβ-FeOOH nanorods wrapped (c) PPNW. (B) Plot of $(\alpha hv)^2$ versus hv for the β-FeOOH nanorods wrapped PPNW. (C) Photoluminescence emission spectra of (a) β-FeOOH powders, (b) β-FeOOH nanorods wrapped PPNW, and (c) β-FeOOH nanorods wrapped PPNW with further deposition of PDA. (D) Suggested mechanism for the enhanced photocatalytic performance of the β-FeOOH nanorods wrapped substrates with PDA as the intermediary layer.

membrane reactor and placed under direct sunlight for 140 min. Colorless water can be filtrated through the porous substrates, and analyses indicate methyl orange has been removed completely.

The photocatalytic performance is also compared between β-FeOOH powders and the immobilized nanorods in the same condition (Figure S12, SI). The degradation efficiency of the β-FeOOH nanorods wrapped substrates is much higher than that of the powders. UV−vis diffuse-reflectance results show that the PDA-coated PPNW has much stronger absorption than the nascent one in the UV and visible region (Figure 6A), which is in accordance with the previous reports.[45] It is worth noting that the β-FeOOH nanorods wrapped PPNW exhibits strong absorption in the visible region from 400 to 600 nm. This means that it has excellent photocatalytic performance in the visible region. The band gap can be acquired for the photocatalyst according to the following equation:[46]

$$\alpha hv = A(hv - E_g)^{n/2} \quad (2)$$

where α, v, h, E_g, and A are absorption coefficient, light frequency, Planck's constant, band gap, and a constant, respectively. In this equation, n can be determined by the type of the transition in a semiconductor (n = 1 for direct transition such as FeOOH[47] and n = 4 for indirect transition). The β-FeOOH nanorods wrapped PPNW has an direct band gap of 1.96 eV by plotting $(\alpha hv)^2$ versus $h\nu$ (Figure 6B), which is less than the reported value of 2.12 eV for β-FeOOH.[27−29] This decrease may be caused by the presence of charge-transfer complexes in which PDA plays a critical role.[48] It is a noteworthy phenomenon that narrow band gap will promote the absorption of visible light and hence improve the photocatalytic performance. In addition, the migration and separation efficiency of photoexcited electron is crucial to the photocatalytic performance.[49] In other words, an excellent photocatalyst should possess high efficiency of charge transfer to decrease the electron−hole recombination rate. Photoluminescence spectra were further used to analyze these phenomena (Figure 6C). The β-FeOOH nanorods wrapped PPNW has a weaker intensity compared with the spectrum of the β-FeOOH powders. It indicates that the β-FeOOH nanorods wrapped substrates have low electron−hole recombination rate. The possible reason is that PDA plays an important role in electron transfer.[14] To reveal the role of PDA, we analyzed the photoluminescence spectra of the β-FeOOH nanorods wrapped PPNW with another 5 h PDA coating, which shows much weaker intensity than the β-FeOOH nanorods wrapped PPNW. It means the photogenerated electrons are easy to inject from the β-FeOOH nanorods into the PDA coating. Therefore, in our cases, PDA can act as an electron acceptor to tune the charge transfer rate and reduce the electron−hole recombination rate.[50] These functions accelerate the kinetics of photocatalytic processes. Figure 6D illustrates a possible mechanism behind the enhancement of photocatalytic performance of the β-FeOOH nanorods on PDA-coated substrates. As we know, β-FeOOH nanorods can react with H_2O_2 to produce ·OH radicals as a photo-Fenton catalyst.[51] In addition, they also produce photogenerated electron−hole pairs under direct sunlight. Then, the electron−hole pairs are separated by the PDA coating which acts as an electron transfer layer. The electrons are rapidly

DOI: 10.1021/acsami.5b02530
ACS Appl. Mater. Interfaces 2015, 7, 11567−11574

captured by H_2O_2 to form tremendously ·OH radicals,[52] which can decompose the organic dyes. This mechanism endows the β-FeOOH nanorods wrapped substrates higher photocatalytic performance than the β-FeOOH powders.

4. CONCLUSION

In conclusion, we have demonstrated a novel strategy to fabricate β-FeOOH nanorods by a mineralization process using various PDA-coated porous materials as a platform. This strategy takes the advantages of PDA coatings such as strong interfacial adhesion, multiple functional groups, and facilitated electron transfer. As a result, the mineralized β-FeOOH nanorods are stably immobilized on the porous substrates, acting as a supported photo-Fenton catalyst. Dyes in water can be efficiently degraded with enhanced photocatalytic performance under direct sunlight. In particular, the photo-Fenton reaction is facilely conjugated with an intermittent membrane reactor for wastewater treatment, which is beneficial for practical application. This work provides an environmentally friendly, energy-saving, and universal method to fabricate photocatalytic materials with high performance.

■ ASSOCIATED CONTENT

Supporting Information

Details of the experiment section, morphologies of the nascent and PDA-coated substrates, stability of the mineral layer after the photo-Fenton reaction, photocatalytic performance of the mineral-coated substrates. The Supporting Information is available free of charge on the ACS Publications website at DOI: 10.1021/acsami.5b02530.

■ AUTHOR INFORMATION

Corresponding Authors

*E-mail: lswan@zju.edu.cn.
*E-mail: xuzk@zju.edu.cn.

Notes

The authors declare no competing financial interest.

■ ACKNOWLEDGMENTS

This work is financially supported by the Zhejiang Provincial Natural Science Foundation of China (Grant No. LZ15E030001) and the National Natural Science Foundation of China (Grant No. 50933006).

■ REFERENCES

(1) Yang, Y.; Li, J. X.; Wang, H.; Song, X. K.; Wang, T. H.; He, B. Q.; Liang, X. P.; Ngo, H. H. An Electrocatalytic Membrane Reactor with Self-Cleaning Function for Industrial Wastewater Treatment. *Angew. Chem., Int. Ed.* **2011**, *50* (9), 2148−2150.

(2) Yu, C. L.; Li, G.; Kumar, S.; Yang, K.; Jin, R. C. Phase Transformation Synthesis of Novel Ag_2O/Ag_2CO_3 Heterostructures with High Visible Light Efficiency in Photocatalytic Degradation of Pollutants. *Adv. Mater.* **2014**, *26* (6), 892−898.

(3) Tusar, N. N.; Maucec, D.; Rangus, M.; Arcon, I.; Mazaj, M.; Cotman, M.; Pintar, A.; Kaucic, V. Manganese Functionalized Silicate Nanoparticles as a Fenton-type Catalyst for Water Purification by Advanced Oxidation Processes (AOP). *Adv. Funct. Mater.* **2012**, *22* (4), 820−826.

(4) Zhou, X. M.; Lan, J. Y.; Liu, G.; Deng, K.; Yang, Y. L.; Nie, G. J.; Yu, J. G.; Zhi, L. J. Facet-Mediated Photodegradation of Organic Dye over Hematite Architectures by Visible Light. *Angew. Chem., Int. Ed.* **2012**, *51* (1), 178−182.

(5) Yurdakal, S.; Loddo, V.; Palmisano, G.; Augugliaro, V.; Berber, H.; Palmisano, L. Kinetics of 4-methoxybenzyl Alcohol Oxidation in Aqueous Solution in a Fixed Bed Photocatalytic Reactor. *Ind. Eng. Chem. Res.* **2010**, *49* (15), 6699−6708.

(6) Meseck, G. R.; Kontic, R.; Patzke, G. R.; Seeger, S. Photocatalytic Composites of Silicone Nanofilaments and TiO_2 Nanoparticles. *Adv. Funct. Mater.* **2012**, *22* (21), 4433−4438.

(7) Lee, J. A.; Krogman, K. C.; Ma, M. L.; Hill, R. M.; Hammond, P. T.; Rutledge, G. C. Highly Reactive Multilayer-Assembled TiO_2 Coating on Electrospun Polymer Nanofibers. *Adv. Mater.* **2009**, *21* (12), 1252−1256.

(8) Liu, B.; Wang, Z.; Dong, Y.; Zhu, Y.; Gong, Y.; Ran, S.; Liu, Z.; Xu, J.; Xie, Z.; Chen, D.; Shen, G. ZnO-Nanoparticle-Assembled Cloth for Flexible Photodetectors and Recyclable Photocatalysts. *J. Mater. Chem.* **2012**, *22* (18), 9379−9384.

(9) Leong, S.; Razmjou, A.; Wang, K.; Hapgood, K.; Zhang, X.; Wang, H. TiO_2 Based Photocatalytic Membranes: A Review. *J. Membr. Sci.* **2014**, *472* (0), 167−184.

(10) Parra, S.; Guasaquillo, I.; Enea, O.; Mielczarski, E.; Mielczarki, J.; Albers, P.; Kiwi-Minsker, L.; Kiwi, J. Abatement of an Azo Dye on Structured C-Nafion/Fe-ion Surfaces by Photo-Fenton Reactions Leading to Carboxylate Intermediates with a Remarkable Biodegradability Increase of the Treated Solution. *J. Phys. Chem. B* **2003**, *107* (29), 7026−7035.

(11) Ma, S.; Meng, J.; Li, J.; Zhang, Y.; Ni, L. Synthesis of Catalytic Polypropylene Membranes Enabling Visible-Light-Driven Photocatalytic Degradation of Dyes in Water. *J. Membr. Sci.* **2014**, *453*, 221−229.

(12) Lopez, L. C.; Buonomenna, M. G.; Fontananova, E.; Iacoviello, G.; Drioli, E.; d'Agostino, R.; Favia, P. A New Generation of Catalytic Poly(vinylidene fluoride) Membranes: Coupling Plasma Treatment With Chemical Immobilization of Tungsten-Based Catalysts. *Adv. Funct. Mater.* **2006**, *16* (11), 1417−1424.

(13) Fontananova, E.; Donato, L.; Drioli, E.; Lopez, L. C.; Favia, P.; d'Agostino, R. Heterogenization of Polyoxometalates on the Surface of Plasma-Modified Polymeric Membranes. *Chem. Mater.* **2006**, *18* (6), 1561−1568.

(14) Rtimi, S.; Nesic, J.; Pulgarin, C.; Sanjines, R.; Bensimon, M.; Kiwi, J., Effect of Surface Pretreatment of TiO_2 Films on Interfacial Processes Leading to Bacterial Inactivation in the Dark and under Light Irradiation. *Interface Focus* **2015**, *5* (1), DOI: 10.1098/rsfs.2014.0046.

(15) Jusoh, R.; Jalil, A. A.; Triwahyono, S.; Idris, A.; Haron, S.; Sapawe, N.; Jaafar, N. F.; Jusoh, N. W. C. Synthesis of Reverse Micelle α-FeOOH Nanoparticles in Ionic Liquid as an Only Electrolyte: Inhibition of Electron-Hole Pair Recombination for Efficient Photoactivity. *Appl. Catal., A* **2014**, *469*, 33−44.

(16) Han, S.; Hu, L.; Liang, Z.; Wageh, S.; Al-Ghamdi, A. A.; Chen, Y.; Fang, X. One-Step Hydrothermal Synthesis of 2D Hexagonal Nanoplates of α-Fe_2O_3/Graphene Composites with Enhanced Photocatalytic Activity. *Adv. Funct. Mater.* **2014**, *24* (36), 5719−5727.

(17) Tada, H.; Mitsui, T.; Kiyonaga, T.; Akita, T.; Tanaka, K. All-Solid-State Z-scheme in CdS-Au-TiO_2 Three-Component Nanojunction System. *Nat. Mater.* **2006**, *5* (10), 782−786.

(18) Lei, P.; Wang, F.; Zhang, S. M.; Ding, Y. F.; Zhao, J. C.; Yang, M. S. Conjugation-Grafted-TiO_2 Nanohybrid for High Photocatalytic Efficiency under Visible Light. *ACS Appl. Mater. Interfaces* **2014**, *6* (4), 2368−2374.

(19) Yang, H. C.; Luo, J. Q.; Lv, Y.; Shen, P.; Xu, Z. K. Surface Engineering of Polymer Membranes via Mussel-Inspired Chemistry. *J. Membr. Sci.* **2015**, *483*, 42−59.

(20) Yang, H. C.; Liao, K. J.; Huang, H.; Wu, Q. Y.; Wan, L. S.; Xu, Z. K. Mussel-Inspired Modification of a Polymer Membrane for Ultra-High Water Permeability and Oil-in-Water Emulsion Separation. *J. Mater. Chem. A* **2014**, *2* (26), 10225−10230.

(21) Ryou, M. H.; Lee, Y. M.; Park, J. K.; Choi, J. W. Mussel-Inspired Polydopamine-Treated Polyethylene Separators for High-Power Li-Ion Batteries. *Adv. Mater.* **2011**, *23* (27), 3066−3070.

(22) Yang, H. C.; Pi, J. K.; Liao, K. J.; Huang, H.; Wu, Q. Y.; Huang, X. J.; Xu, Z. K. Silica-Decorated Polypropylene Microfiltration Membranes with a Mussel-Inspired Intermediate Layer for Oil-in-

DOI: 10.1021/acsami.5b02530
ACS Appl. Mater. Interfaces 2015, 7, 11567−11574

Water Emulsion Separation. *ACS Appl. Mater. Interfaces* **2014**, *6* (15), 12566−12572.
(23) Chen, P. C.; Wan, L. S.; Xu, Z. K. Bio-Inspired $CaCO_3$ Coating for Superhydrophilic Hybrid Membranes with High Water Permeability. *J. Mater. Chem.* **2012**, *22* (42), 22727−22733.
(24) Chen, P. C.; Xu, Z. K. Mineral-Coated Polymer Membranes with Superhydrophilicity and Underwater Superoleophobicity for Effective Oil/Water Separation. *Sci. Rep.* **2013**, *3*, 2776.
(25) Kim, J. H.; Lee, M.; Park, C. B. Polydopamine as a Biomimetic Electron Gate for Artificial Photosynthesis. *Angew. Chem., Int. Ed.* **2014**, *53* (25), 6364−6368.
(26) Dimitrijevic, N. M.; Rozhkova, E.; Rajh, T. Dynamics of Localized Charges in Dopamine-Modified TiO_2 and Their Effect on the Formation of Reactive Oxygen Species. *J. Am. Chem. Soc.* **2009**, *131* (8), 2893−2899.
(27) Xiong, Y.; Xie, Y.; Chen, S.; Li, Z. Fabrication of Self-Supported Patterns of Aligned β-FeOOH Nanowires by a Low-Temperature Solution Reaction. *Chem. - Eur. J.* **2003**, *9* (20), 4991−4996.
(28) Zhao, Y.; Jiangyong, H.; Chen, H. Elimination of Estrogen and Its Estrogenicity by Heterogeneous Photo-Fenton Catalyst β-FeOOH/Resin. *J. Photochem. Photobiol., A* **2010**, *212* (2), 94−100.
(29) Xu, Z.; Zhang, M.; Wu, J.; Liang, J.; Zhou, L.; L, B. Visible Light-Degradation of Azo Dye Methyl Orange Using TiO_2/β-FeOOH as a Heterogeneous Photo-Fenton-Like Catalyst. *Water Sci. Technol.* **2013**, *68* (10), 2178−2185.
(30) Sever, M. J.; Weisser, J. T.; Monahan, J.; Srinivasan, S.; Wilker, J. J. Metal-Mediated Cross-Linking in the Generation of a Marine-Mussel Adhesive. *Angew. Chem., Int. Ed.* **2004**, *43* (4), 448−450.
(31) Lee, H.; Dellatore, S. M.; Miller, W. M.; Messersmith, P. B. Mussel-Inspired Surface Chemistry for Multifunctional Coatings. *Science* **2007**, *318* (5849), 426−430.
(32) Milosevic, I.; Jouni, H.; David, C.; Warmont, F.; Bonnin, D.; Motte, L. Facile Microwave Process in Water for the Fabrication of Magnetic Nanorods. *J. Phys. Chem. C* **2011**, *115* (39), 18999−19004.
(33) Abidi, N.; Cabrales, L.; Hequet, E. Functionalization of a Cotton Fabric Surface with Titania Nanosols: Applications for Self-Cleaning and UV-Protection Properties. *ACS Appl. Mater. Interfaces* **2009**, *1* (10), 2141−2146.
(34) Wei, C. Z.; Nan, Z. D. Effects of Experimental Conditions on One-Dimensional Single-Crystal Nanostructure of β-FeOOH. *Mater. Chem. Phys.* **2011**, *127* (1−2), 220−226.
(35) Chen, M. L.; Shen, L. M.; Chen, S.; Wang, H.; Chen, X. W.; Wang, J. H. In Situ Growth of β-FeOOH Nanorods on Graphene Oxide with Ultra-high Relaxivity for in Vivo Magnetic Resonance Imaging and Cancer Therapy. *J. Mater. Chem. B* **2013**, *1* (20), 2582−2589.
(36) Fernandez, J.; Bandara, J.; Lopez, A.; Buffat, P.; Kiwi, J. Photoassisted Fenton Degradation of Nonbiodegradable Azo Dye (Orange II) in Fe-Free Solutions Mediated by Cation Transfer Membranes. *Langmuir* **1999**, *15* (1), 185−192.
(37) Dhananjeyan, M. R.; Mielczarski, E.; Thampi, K. R.; Buffat, P.; Bensimon, M.; Kulik, A.; Mielczarski, J.; Kiwi, J. Photodynamics and Surface Characterization of TiO_2 and Fe_2O_3 Photocatalysts Immobilized on Modified Polyethylene Films. *J. Phys. Chem. B* **2001**, *105* (48), 12046−12055.
(38) Anpo, M.; Thomas, J. M. Single-Site Photocatalytic Solids for the Decomposition of Undesirable Molecules. *Chem. Commun.* **2006**, *31*, 3273−3278.
(39) Wu, Z.; Sheng, Z.; Liu, Y.; Wang, H.; Mo, J. Deactivation Mechanism of PtOx/TiO_2 Photocatalyst towards the Oxidation of NO in Gas Phase. *J. Hazard. Mater.* **2011**, *185* (2), 1053−1058.
(40) Zhang, L.; Chen, L.; Xiao, M.; Zhang, L.; Wu, F.; Ge, L. Enhanced Decolorization of Orange II Solutions by the Fe(II)-Sulfite System under Xenon Lamp Irradiation. *Ind. Eng. Chem. Res.* **2013**, *52* (30), 10089−10094.
(41) Feng, J. Y.; Hu, X. J.; Yue, P. L.; Zhu, H. Y.; Lu, G. Q. Degradation of Azo-Dye Orange II by a Photoassisted Fenton Reaction Using a Novel Composite of Iron Oxide and Silicate Nanoparticles as a Catalyst. *Ind. Eng. Chem. Res.* **2003**, *42* (10), 2058−2066.
(42) Ramirez, J. H.; Maldonado-Hodar, F. J.; Perez-Cadenas, A. F.; Moreno-Castilla, C.; Costa, C. A.; Madeira, L. M. Azo-dye Orange II degradation by heterogeneous Fenton-like reaction using carbon-Fe catalysts. *Appl. Catal., B* **2007**, *75* (3−4), 312−323.
(43) Cao, Q.; Che, R.; Chen, N. Facile and Rapid Growth of Ag_2S Microrod Arrays as Efficient Substrates for Both SERS Detection and Photocatalytic Degradation of Organic Dyes. *Chem. Commun.* **2014**, *50* (38), 4931−4933.
(44) Gao, S. Y.; Cao, R.; Lu, J.; Li, G. L.; Li, Y. F.; Yang, H. X. Photocatalytic Properties of Polyoxometalate-Thionine Composite Films Immobilized onto Microspheres under Sunlight Irradiation. *J. Mater. Chem.* **2009**, *19* (24), 4157−4163.
(45) Yang, H. C.; Wu, Q. Y.; Wan, L. S.; Xu, Z. K. Polydopamine Gradients by Oxygen Diffusion Controlled Autoxidation. *Chem. Commun.* **2013**, *49* (89), 10522−10524.
(46) Yao, W. F.; Huang, C. P.; Ye, J. H. Hydrogen Production and Characterization of $MLaSrNb_2NiO_9$ (M = Na, Cs, H) Based Photocatalysts. *Chem. Mater.* **2010**, *22* (3), 1107−1113.
(47) Chemelewski, W. D.; Rosenstock, J. R.; Mullins, C. B. Electrodeposition of Ni-doped FeOOH Oxygen Evolution Reaction Catalyst for Photoelectrochemical Water Splitting. *J. Mater. Chem. A* **2014**, *2* (36), 14957−14962.
(48) de la Garza, L.; Saponjic, Z. V.; Dimitrijevic, N. M.; Thurnauer, M. C.; Rajh, T. Surface States of Titanium Dioxide Nanoparticles Modified with Enediol Ligands. *J. Phys. Chem. B* **2006**, *110* (2), 680−686.
(49) Lee, J. S.; You, K. H.; Park, C. B. Highly Photoactive, Low Bandgap TiO_2 Nanoparticles Wrapped by Graphene. *Adv. Mater.* **2012**, *24* (8), 1084−1088.
(50) Kamat, P. V. Boosting the Efficiency of Quantum Dot Sensitized Solar Cells throughModulation of Interfacial Charge Transfer. *Acc. Chem. Res.* **2012**, *45* (11), 1906−1915.
(51) Yuan, B.; Xu, J.; Li, X.; Fu, M. L. Preparation of Si-Al/α-FeOOH Catalyst from an Iron-Containing Waste and Surface-Catalytic Oxidation of Methylene Blue at Neutral pH Value in the Presence of H_2O_2. *Chem. Eng. J.* **2013**, *226* (0), 181−188.
(52) Ge, M.; Liu, L.; Chen, W.; Zhou, Z. Sunlight-Driven Degradation of Rhodamine B by Peanut-Shaped Porous $BiVO_4$ Nanostructures in the H_2O_2-Containing System. *CrystEngComm* **2012**, *14* (3), 1038−1044.

DOI: 10.1021/acsami.5b02530
ACS Appl. Mater. Interfaces 2015, 7, 11567−11574